Title

Type 1 diabetes immunotherapy using polyclonal regulatory T cells

Authors

Bluestone, Jeffrey A
Buckner, Jane H
Fitch, Mark
et al.

IMMUNOTHERAPY

Type 1 diabetes immunotherapy using polyclonal regulatory T cells

Jeffrey A. Bluestone,[1]* Jane H. Buckner,[2] Mark Fitch,[3] Stephen E. Gitelman,[4] Shipra Gupta,[2] Marc K. Hellerstein,[3] Kevan C. Herold,[5] Angela Lares,[1] Michael R. Lee,[1] Kelvin Li,[6] Weihong Liu,[1] S. Alice Long,[2] Lisa M. Masiello,[1] Vinh Nguyen,[7] Amy L. Putnam,[1] Mary Rieck,[1] Peter H. Sayre,[8] Qizhi Tang[7]

Type 1 diabetes (T1D) is an autoimmune disease that occurs in genetically susceptible individuals. Regulatory T cells (T_{regs}) have been shown to be defective in the autoimmune disease setting. Thus, efforts to repair or replace T_{regs} in T1D may reverse autoimmunity and protect the remaining insulin-producing β cells. On the basis of this premise, a robust technique has been developed to isolate and expand T_{regs} from patients with T1D. The expanded T_{regs} retained their T cell receptor diversity and demonstrated enhanced functional activity. We report on a phase 1 trial to assess safety of T_{reg} adoptive immunotherapy in T1D. Fourteen adult subjects with T1D, in four dosing cohorts, received ex vivo–expanded autologous $CD4^+CD127^{lo/-}CD25^+$ polyclonal T_{regs} (0.05×10^8 to 26×10^8 cells). A subset of the adoptively transferred T_{regs} was long-lived, with up to 25% of the peak level remaining in the circulation at 1 year after transfer. Immune studies showed transient increases in T_{regs} in recipients and retained a broad T_{reg} $FOXP3^+CD4^+CD25^{hi}CD127^{lo}$ phenotype long-term. There were no infusion reactions or cell therapy–related high-grade adverse events. C-peptide levels persisted out to 2+ years after transfer in several individuals. These results support the development of a phase 2 trial to test efficacy of the T_{reg} therapy.

INTRODUCTION

Type 1 diabetes (T1D) is an autoimmune disease that occurs in genetically susceptible individuals, influenced by the environment and stochastic events (1). These conditions result in immune dysregulation, leading to the generation of pathogenic T cells and destruction of β cells in the islets of Langerhans. T1D is one of the most prevalent chronic diseases of childhood. Despite advances in insulin formulations, insulin delivery systems, and glucose monitoring, less than one-third of patients meet clinical care targets needed to prevent secondary end-organ complications such as retinal, renal, and neurological disease (2, 3). Thus, it is not surprising that the past two decades of research have focused on developing new therapeutics to prevent and treat this devastating disease. Several immunomodulatory therapies, including anti-CD3 (teplizumab) (4), LFA3Ig (alefacept) (5), and anti-thymocyte globulin (thymoglobulin) in combination with granulocyte colony-stimulating factor with or without cyclophosphamide (6), and bone marrow transplantation (6, 7), have shown some promise for the treatment of T1D, yet none has induced permanent immune tolerance (that is, nonresponsiveness to self-tissues or foreign tissues without the need for continuous immune suppression) or resulted in long-term insulin independence. However, one common finding that has emerged from these studies is that the major immunomodulatory effect was to induce, or preferentially support, a regulatory T cell (T_{reg}) subset that is likely to be responsible for the drug efficacy (8). Indeed, this key discovery has

provided increased emphasis on the development of T_{reg} and T_{reg}-supportive therapies for the treatment of this challenging disease.

T_{regs} were initially described as a population of $CD4^+CD25^+$ T cells that are critical for controlling autoimmunity and tolerance (9, 10). T_{regs} inhibit effector T cell (T_{eff}) responses both in vitro and in vivo through a variety of activities including cell-cell contact and soluble factors (11). The identification of the transcription factor FOXP3 as a lineage marker for T_{regs} has been instrumental in advancing the field. Mutations or deficiency in the FOXP3 gene in scurfy mice or immuno-dysregulation polyendocrinopathy enteropathy X-linked syndrome (IPEX) patients results in a reduced and/or nonfunctional T_{reg} compartment, leading to a fatal multiorgan autoimmune disease (12). FOXP3 controls many aspects of T_{reg} biology, including their development, transcriptional program, and suppressive function in vitro and in vivo. Thus, $CD4^+CD25^+FOXP3^+$ T_{regs} are an essential immunosuppressive cell population for the extrinsic control of immune homeostasis and control of autoimmunity and have a unique and highly robust therapeutic profile. Although T_{regs} require specific T cell receptor (TCR)–mediated activation to develop regulatory activity, their effector function regulates local inflammatory responses through a combination of cell-cell contact and suppressive cytokine production (11, 13, 14). Thus, T_{regs} specific for a limited number of antigens can efficiently suppress a polyclonal autoreactive response due to dominant antigen nonspecific immuno-regulation termed "bystander suppression." Moreover, activated T_{regs} can recruit additional regulatory cell populations through a process termed infectious tolerance to achieve long-lasting disease protection (14). There is increasing evidence in mouse models that the adoptive transfer (AT) of T_{regs} in multiple disease settings, including T1D, results in disease prevention and, in many cases, disease remission (15, 16). Recently, we and others have shown that T_{regs} are defective in a wide variety of autoimmune diseases, including T1D (17). These defects are manifested by loss of T_{reg} number in inflamed tissues, reduced signaling through the interleukin-2 (IL-2) receptor [based on reduced signal

[1]Diabetes Center, University of California, San Francisco, San Francisco, CA 94143, USA. [2]Translational Research Program, Benaroya Research Institute at Virginia Mason, Seattle, WA 98101, USA. [3]Department of Nutritional Sciences and Toxicology, University of California, Berkeley, Berkeley, CA 94720, USA. [4]Department of Pediatrics, University of California, San Francisco, San Francisco, CA 94143, USA. [5]Departments of Immunobiology and Internal Medicine, Yale University School of Medicine, New Haven, CT 06520, USA. [6]KineMed Inc., Emeryville, CA 94608, USA. [7]Department of Surgery, University of California, San Francisco, San Francisco, CA 94143, USA. [8]Division of Hematology-Oncology, Department of Medicine, University of California, San Francisco, San Francisco, CA 94143, USA.
*Corresponding author. E-mail: jeff.bluestone@ucsf.edu

transducer and activator of transcription 5 (STAT5) phosphorylation], and instability of the suppressive activities of the cells in vitro and in vivo (18). These observations have opened an important new concept of drug intervention in autoimmunity, namely, T_{regs} as immunotherapeutics, particularly if the abnormalities observed in T_{regs} in vivo can be corrected through their expansion.

Unlike mice, isolation of T_{regs} based on the CD4 and CD25 markers is not sufficient to isolate most of the FOXP3$^+$ T_{regs} without the risk of contamination with potentially autoreactive T_{effs}. We have shown that a combination of cell surface markers—CD4, CD25, and CD127—provides a robust cocktail to isolate FOXP3$^+$ T_{regs} by fluorescence-activated cell sorting (FACS) from peripheral blood of subjects with T1D (19). On the basis of this selection method, we developed a clinical-scale expansion process for obtaining, in many instances, greater than 3×10^9 T_{regs} after in vitro expansion of cells sorted from peripheral blood lymphocytes from a single donor (20).

Here, we describe the results of a phase 1 trial in recent-onset T1D. The study included four dosing cohorts (a total of 14 adult patients) that received expanded polyclonal T_{regs} (polyT_{regs}) ranging from ~5×10^6 to ~2.6×10^9 cells in a single infusion. The expansion process resulted in T_{regs} with enhanced STAT5 phosphorylation in response to IL-2, increased T_{reg} suppressive activity in vitro, and long-term survival in vivo (greater than 1 year). The cell therapy was well tolerated with no evidence of short-term toxicities (including infusion reactions or cytokine release syndrome), precipitous decline in endogenous insulin production, or opportunistic infections.

RESULTS

Study design

The trial was a phase 1, two-center, open-label, dose-escalation study conducted at the University of California, San Francisco (UCSF) and Yale University in which participants with recent-onset T1D received a single infusion of ex vivo–expanded autologous CD4$^+$CD127$^{lo/-}$CD25$^+$ polyT_{regs} in four dosing cohorts (Fig. 1). The first subject in each cohort was observed for 3 weeks after infusion, after which time the study team met to review cumulative safety data. If no grade 3 or higher adverse event was observed, subsequent subjects in that cohort could be treated. After the 13-week follow-up visit of the last subject in each cohort, an independent data and safety monitoring board (DSMB) reviewed cumulative safety data for approval to escalate the dose and progress to the next cohort. Primary outcome measures were adverse events, laboratory abnormalities, and other signs of toxicity. Secondary diabetes-related outcome measures included C-peptide response during mixed meal tolerance tests (MMTTs), insulin use, and hemoglobin A1c (HbA1c). Figure 1 highlights the schedule of events that includes relevant time points for patient blood sampling for various assessments described below. Table 1 describes the endpoints for the study as defined. This study was approved by institutional review boards at UCSF and Yale University and is registered with ClinicalTrials.gov (NCT01210664).

Patient characteristics

Twenty-six patients were screened, 16 met eligibility criteria and were enrolled, and 14 subjects received a single infusion of polyT_{regs}. Table 2 shows the demographic and baseline characteristics of the treated subjects. Of the 14 treated subjects, 6 were female and 8 were
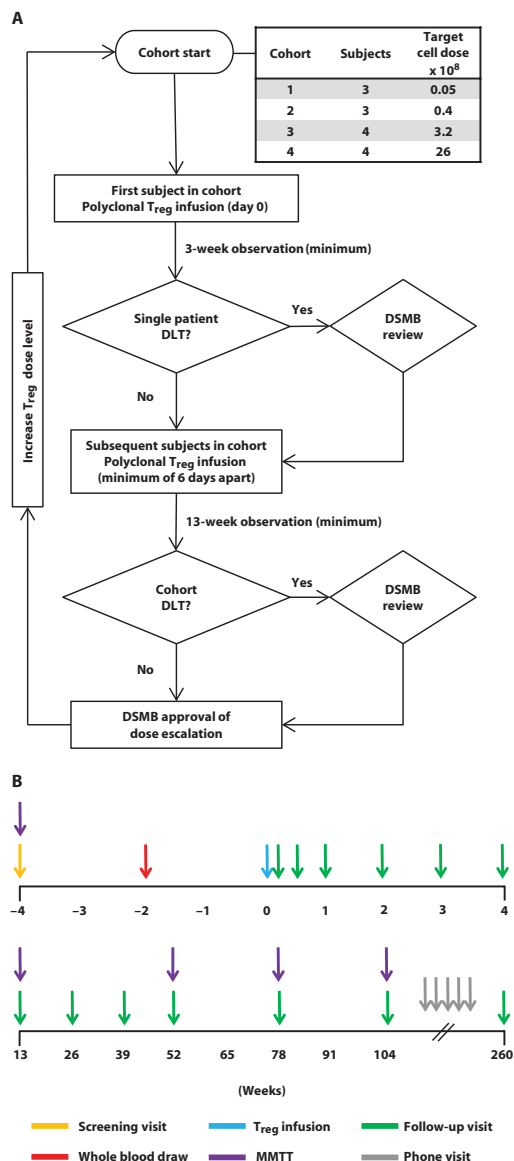
Fig. 1. Study design. (A) Dose escalation plan. Subjects were enrolled in four cohorts with target doses ranging from 0.05×10^8 to 26×10^8, where the dose was escalated by eightfold for each subsequent cohort. The first subject in each cohort received a single infusion of polyT_{regs} and was observed for a minimum of 3 weeks for dose-limiting toxicities (DLT), after which time clinical data were extracted from the database and study team safety review was conducted. If no grade 3 or higher adverse event was observed, treatment of subsequent subjects in that cohort could proceed. Otherwise, treatment would be suspended for DSMB review. After treatment of the last subject in each cohort, subjects were observed for a minimum of 13 weeks. The study team reviewed cumulative data to assess for any grade 3 or higher related adverse event, any related serious adverse event, undetectable C-peptide in an MMTT at week 13 in two subjects, or any other significant safety concerns based on other considerations. The study team's review decision was reported to the DSMB for approval before proceeding to the next dosing cohort. **(B)** Subject schedule of events. Blood (target of 400 ml) for T_{reg} manufacturing was drawn at week −2, and T_{reg} infusion was given on day 0. Subjects were seen for follow-up assessments on day 4, then weekly for the first 4 weeks, then every 13 weeks for the first year, and then every 6 months for 2 years, and contacted by phone every 6 months for years 3 to 5 to assess for adverse events.

male. The mean age was 30.3 ± 8.7 years, and the mean disease duration was 39 ± 26.4 weeks at the time of screening. The mean follow-up at the time of data cutoff for this article was 124 weeks (cohort 1: 182 weeks; cohort 2: 156 weeks; cohort 3: 104 weeks; and cohort 4: 78 weeks). The two subjects who did not receive expanded T_{regs} were not included in the data analysis.

Table 1. Primary and secondary study objectives and endpoints.

Objectives	Endpoints
Primary objective	Primary endpoints
Assess the safety and feasibility of intravenous infusion of ex vivo–selected and ex vivo–expanded autologous polyT$_{regs}$ in patients with T1D	Adverse events
	Laboratory abnormalities
	Signs of toxicity
	Infusion reactions
	Complications related to infection
	Potential negative impact on the course of diabetes
Secondary objectives	Secondary endpoints
Effects on endogenous insulin secretion: Assess the effect of T$_{regs}$ on β cell function and on other measures of diabetes severity	C-peptide response during MMTTs
	Insulin use
	HbA1c
Surrogate markers of diabetes immune response: Measure the effect of T$_{regs}$ on the pathologic autoimmune response underlying T1D and on general immune responsiveness	Secondary surrogate immunologic markers related to general immune function and diabetes autoimmune response

T_{reg} isolation and expansion

We have established a robust selection and expansion method for polyT$_{regs}$ from individuals with T1D, where three cell surface markers—CD4, CD25, and CD127—were used to FACS purify the FOXP3$^+$ T$_{regs}$ present in the peripheral blood as described previously (20). Purified T$_{regs}$ were cultured with clinical-grade Dynabeads coated with anti-CD3 and anti-CD28 plus recombinant IL-2. As seen in Table 3, a unit of blood yielded between 4.2×10^6 and 11.8×10^6 purified CD4$^+$ CD127$^{lo/-}$CD25$^+$ T$_{regs}$, which on average expanded 554.7 ± 370.2–fold (SD) (ranging from 29.8-fold to 1366.8-fold), with each incremental cohort averaging a greater fold expansion as our experience progressed (Table 3). The expression of FOXP3 has been the most reliable marker of T$_{regs}$. On average, the expanded T$_{reg}$ preparations that were infused were 92.2% FOXP3$^+$ (range, 76 to 96.9%), with only two preparations <90% positive. The T$_{reg}$ preparations met the additional release criteria of high viability (cutoff ≥85%, actual >98%), high CD4$^+$ percentage (≥95%), and low CD8$^+$ cell contamination (cutoff ≤5%, actual <2.5%) (Table 4). Of 16 attempted expansions, two preparations of expanded T$_{regs}$ did not meet release criteria. The cell preparation for patient 002-011 had a population (7.36%) of CD4$^+$CD8$^+$ "double-positive" T$_{regs}$ in the expanded population, which exceeded the release criterion of ≤5% CD8$^+$ cells. However, follow-up analyses showed that the double-positive cells were FOXP3$^+$, did not change during the culture period, and suppressed efficiently in vitro. Moreover, the percentage of double-positive cells did not change during the culture period, suggesting that these cells were indeed present in the circulation of this donor, perhaps representing a small population of tissue-derived T$_{regs}$ as has been suggested for T$_{effs}$ previously (21). Preparation for patient 007-014 contained a population of CD4$^+$ T$_{effs}$ in the expanded cultures (about 80%). Subsequent studies showed that the T$_{eff}$ "contamination" was due to a low level of expression of CD127 on T$_{effs}$, making it difficult, with current clinical-grade anti-CD127 monoclonal antibodies, to completely separate the T$_{eff}$ from T$_{reg}$ even after CD4 and CD25 gating.

Table 2. Subject characteristics. Subjects are listed in order of enrollment.

	Subject ID	Age at enrollment (years)	Sex	Time from diagnosis at screening (weeks)	HbA1c at screening (%)
1	002-002	35	F	17	6.4
	002-003	26	M	19	4.9
	002-004	32	M	20	5.3
2	002-005	35	F	86	5.7
	002-007	40	M	30	5.2
	002-008	32	M	14	6.0
3	007-101	19	M	30	6.0
	002-015	43	M	104	5.3
	007-102	21	F	42	9.9
	002-017	24	M	29	7.1
4	002-018	43	M	27	7.0
	002-019	34	F	52	6.5
	007-103	18	F	28	6.2
	002-022	22	F	42	4.7

Table 3. Initial T$_{reg}$ purity and expansion. The number of T$_{regs}$ isolated from ~400 ml of whole blood, the T$_{reg}$ purity (%CD4$^+$CD127$^{lo/−}$CD25$^+$) after FACS, total number of T$_{regs}$ after 14-day expansion, fold increase from number of T$_{regs}$ seeded, and the total number of T$_{regs}$ infused.

Cohort	Subject ID	Number of T$_{regs}$ before expansion (×10^6)	T$_{reg}$ purity (%)	Number of T$_{regs}$ after expansion (×10^9)	Fold expansion	Number of T$_{regs}$ infused (×10^8)
1	002-002	6.5	99.6	0.96	148.9	0.056
	002-003	6.3	98.7	0.19	29.8	0.050
	002-004	6.8	98.7	1.34	197.7	0.056
2	002-005	4.2	98.8	1.35	322.2	0.436
	002-007	4.5	97.9	2.57	576.8	0.425
	002-008	6.0	99.1	3.05	505.0	0.398
3	007-101	5.4	97.3	2.96	544.8	3.81
	002-015	5.8	98.1	2.70	495.9	3.46
	007-102	8.0	99.2	11.0	1366.8	3.68
	002-017	6.3	99.4	3.11	518.1	3.31
4	002-018	10.4	96.3	13.0	1242.4	26.8
	002-019	11.8	98.5	7.20	613.2	26.9
	007-103	6.3	97.9	3.30	527.1	29.4
	002-022	4.7	98.1	3.20	677.2	23.5

Table 4. Final T$_{reg}$ release specifications and results. Final cell product was assessed for identity (≥60% FOXP3$^+$ and ≥95% CD4$^+$ cells), purity (≤5% CD8$^+$ cells, <100 beads per 3 × 10^6 cells, and endotoxin ≤3.5 EU/ml), sterility (negative for mycoplasma, anaerobic and aerobic bacteria, gram stain, fungal culture, KOH exam), and viability (≥85%).

	Result (%) (subject ID)													
	Cohort 1			Cohort 2			Cohort 3				Cohort 4			
Assay (specification)	(002-002)	(002-003)	(002-004)	(002-005)	(002-007)	(002-008)	(007-101)	(002-015)	(007-102)	(002-017)	(002-018)	(002-019)	(007-103)	(002-022)
Percentage of FOXP3$^+$ cells (≥60%)	76.0	92.0	95.6	82.6	96.8	94.2	94.3	96.9	92.4	93.8	94.0	95.3	94.9	92.0
Percentage of CD4$^+$ cells (≥95%)	96.0	95.0	97.3	95.2	98.5	98.7	98.5	98.3	97.9	97.3	98.4	97.5	98.2	96.5
Percentage of CD8$^+$ cells (≤5%)	2.4	1.9	0.8	0.1	0.2	0.1	0.1	0.6	0.1	0.9	0.36	0.20	0.59	0.40
Viability (≥85%)	100	99.5	98.5	98.5	99.0	99.4	98.7	99.8	99.4	99.3	99.3	98.6	99.0	99.3

Phenotypic and TCR analysis of expanded polyT$_{regs}$

Key cell surface markers, CD4 and CD127, used to isolate the T$_{regs}$ were largely unchanged after expansion, although CD25 expression increased, which reflected the feedback induction caused by culturing the cells with IL-2. Our previous data demonstrated that the naïve CD45RA$^+$ T$_{regs}$ preferentially expand in the cultures; however, the CD45RA$^+$RO$^−$ cells down-regulate CD45RA and up-regulate CD45RO$^+$ over the expansion period (20). An example is shown in Fig. 2A, where the percent CD45RO$^+$ T$_{regs}$ went from 52% before culture to 97% after

culture. In addition, the cell expansion led to up-regulation of the cell surface markers CCR7 and CD38 increasing from 67% and 8% fresh, to 98% and 97% in expanded populations, respectively (Fig. 2, B and C). CCR7 has been shown to enhance T$_{reg}$ trafficking to lymph nodes (22). CD38, a multifunctional ectoenzyme that catalyzes the synthesis and hydrolysis of cyclic adenosine diphosphate (ADP)–ribose from nicotinamide adenine dinucleotide (NAD$^+$) to ADP-ribose, is reported to be essential for the regulation of intracellular Ca^{2+} and associated with enhanced T$_{reg}$ function (23). A summary of all the tested patients for

each marker is included on the right panels of Fig. 2. These data (right panels) suggest that the potent activation induced in vitro by anti-CD3, anti-CD28, and IL-2 led to a highly activated phenotype with the potential for enhanced T_{reg} function in vivo. The TCRβ repertoire of the expanded T_{regs} was analyzed and compared to the freshly isolated populations to determine the polyclonality of the expanded T_{regs}. The expanded cells exhibited polyclonality indistinguishable from the preexpansion cultures based on high-throughput TCRβ sequencing (Adaptive Biotechnologies) (fig. S1), suggesting that the T_{regs} remained a highly diverse population after expansion.

Functional analysis of expanded polyT$_{regs}$

FOXP3 protein can increase transiently in T_{effs} in response to activation signals. However, the DNA methylation state of enhancer region of the FOXP3 locus [T_{reg}-specific demethylated region (TSDR)] remains methylated in all but bona fide T_{regs} (24). We analyzed methylation of each preparation. The FOXP3 TSDR remained demethylated in the expanded T_{regs}, and FOXP3 protein levels correlated with overall demethylation status at the FOXP3 TSDR, indicating overall purity and stability of the expanded T_{regs} (Fig. 3A).

Impaired function of T_{regs} in patients with T1D has been ascribed to a reduced phosphorylation of STAT5 (pSTAT5) in response to IL-2
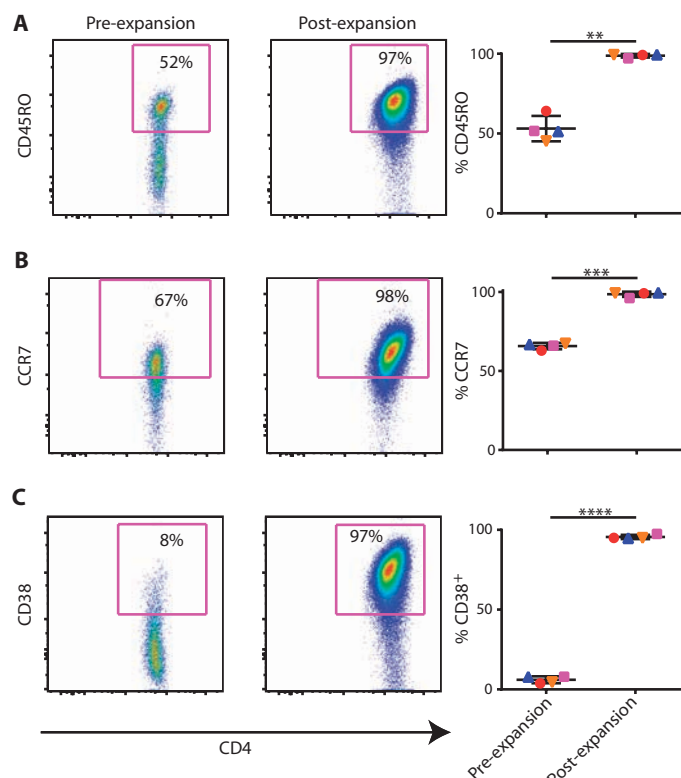
Fig. 2. Increased expression of CD45RO, CCR7, and CD38 on T$_{regs}$ after in vitro expansion. (**A** to **C**) CD4$^+$CD25$^+$CD127^{lo} T$_{regs}$, as shown in fig. S6, were stained for (A) CD45RO, (B) CCR7, and (C) CD38 before and after expansion. Representative FACS plots are shown for each of these stains on the left, and graphs plotting data for all subjects ($n = 4$) on the right. Data points for each subject are represented in a unique and consistent symbol (blue upright triangle, red circle, orange inverted triangle, and magenta square). **$P = 0.0014$, ***$P = 0.0001$, ****$P < 0.0001$, paired t test.

(18). pSTAT5 is a key transcription factor essential for IL-2–driven T_{reg} expansion and survival. Exposure to IL-2 in vivo results in an improvement of IL-2–driven pSTAT5 (25), suggesting that ex vivo expansion of T_{reg} with high-dose IL-2 could enhance the IL-2 response in T1D T_{reg}. Indeed, we found that after 14 days of expansion with IL-2, T1D T_{regs} demonstrate an increase in pSTAT5 in response to IL-2 ($P = 0.0185$), a finding that is most profound in the T_{reg} that had an IL-2 (pSTAT5) level below the mean of T_{reg} from controls (paired t test = 0.0024) (Fig. 3B). Notably, after 14 days of expansion, the response to IL-2 was not different from T_{regs} from between T1D patients and healthy control subjects. This was unrelated to the relative expression of CD25 but reflected changes in the signaling through the TCR, CD28, and CD25 cell surface receptors.

We have previously described T_{reg} "instability" in patients with T1D based on our identification of their production of interferon-γ (IFN-γ), a T helper 1 ($T_{H}1$)–type effector molecule that has been ascribed to participate in the pathogenesis of disease (26), and other studies have shown that expanded T_{regs} can begin to produce type 2 cytokines such as IL-4 and IL-5 (27, 28). Therefore, we examined supernatants harvested from in vitro expansion cultures and ex vivo–expanded T_{regs} stimulated overnight with phorbol 12-myristate 13-acetate (PMA) and ionomycin and analyzed for type 1 and 2 cytokines by cytometric bead array (Becton Dickinson) to determine how the expansion had affected their function. Similar to our previous studies (20), there were only a limited amount of T_{eff} cytokines (that is, IFN-γ and IL-17) produced in the culture, and the levels of these cytokines did not change after ex vivo expansion based on intracellular flow cytometric or culture supernatants analyses.

Finally, we examined the suppressive activity of the expanded T_{regs} in vitro. Initial studies were performed using fresh versus expanded T_{regs} from a series of healthy individuals. The expanded T_{regs} routinely suppressed the PBMC proliferation at significantly lower conventional T cell (T_{conv})/T_{reg} ratios than the nonexpanded cells (Fig. 3C). Similarly, analysis of three expanded T_{reg} preparations from patients in the phase 1 trial demonstrated four- to eightfold greater suppressive activity than nonexpanded T_{regs} from the same individual (Fig. 3D). Overall, the expanded T_{regs} from the 14 patients in the phase 1 trial demonstrated suppressive activity greater than 50% at ratios of 1:32 T_{conv}/T_{reg} or lower, which suggested overall greater activity by the expanded versus nonexpanded T_{regs} (fig. S2). Finally, we examined a series of cell surface and functional markers on the nonexpanded versus expanded T_{regs} (Fig. 3E). In addition to the increased suppressive activity, the expanded T_{regs} showed significant increases in the expression of CD25, CTLA-4, and LAP, all of which have been shown to be involved in T_{reg} function (11, 14, 29). Together, the phenotypic and functional data suggest that the expansion of the T_{regs} increased not only the overall number of cells for AT but also the functional potential of these cells on a per-cell basis.

Safety

All patients received the target dose according to dose escalation cohort (Table 3). A tabulated cumulative summary of adverse events for all cohorts categorized by system organ class and severity is listed in table S1. There were no infusion reactions. After a mean follow-up of 31 months, there were 11 grade 3 or 4 adverse events, which largely reflected metabolic abnormalities of underlying diabetes. Four serious adverse events were reported. One patient had three episodes of serious hypoglycemia 14, 248, and 463 days after T_{reg} infusion in one subject and one episode of diabetic ketoacidosis 67 days after T_{reg} infusion in a second subject.
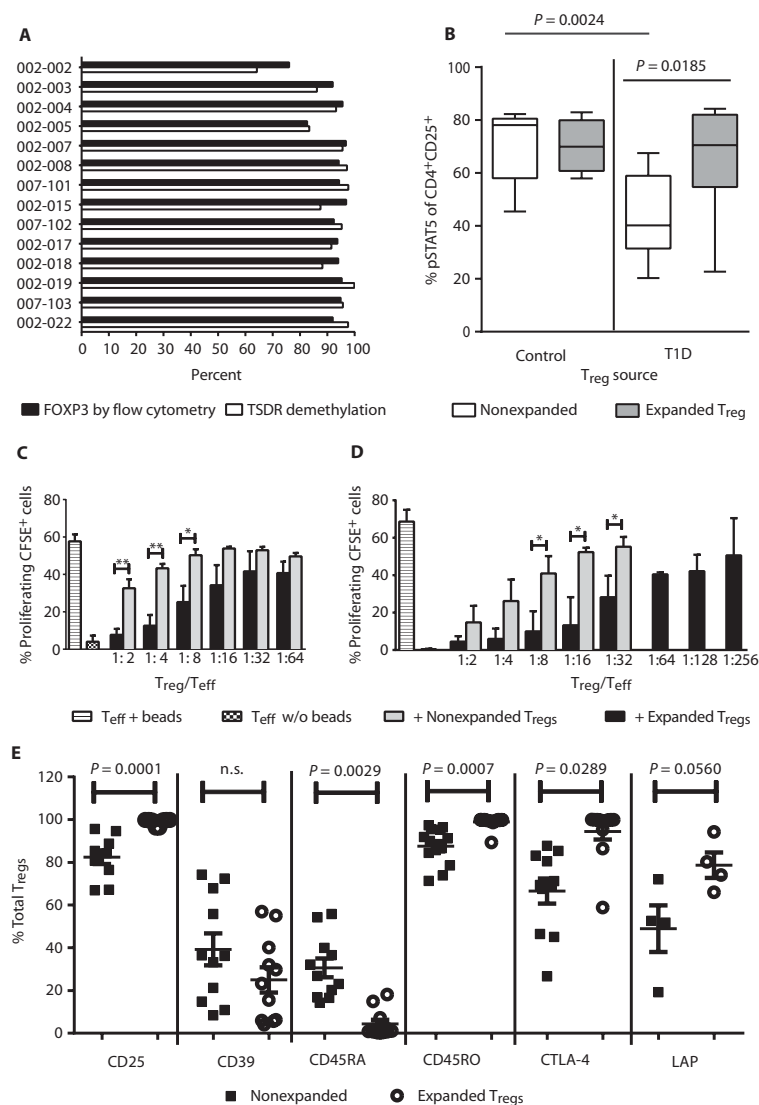
Fig. 3. T_reg identity and function. (**A**) Percent of expanded cells expressing FOXP3 protein was determined by flow cytometry, and percent of DNA demethylated at the FOXP3 TSDR was determined by Epiontis as described in Materials and Methods. (**B**) Percent of STAT5 phosphorylation in response to IL-2 stimulation in CD4$^+$CD25$^+$ T_regs before and after expansion in healthy controls ($n = 5$) and subjects with T1D ($n = 10$). Staining and gating were done as previously described (25). Significance was determined by the Mann-Whitney test. (**C**) In an in vitro culture, carboxyfluorescein diacetate succinimidyl ester (CFSE)–labeled T_effs were cultured for 4 days in the presence of anti-CD3/CD28 antibody–coated beads in the presence or absence of expanded/natural T_regs of the same donor. T cell proliferation in these cultures was analyzed by flow cytometry for CFSE dilution as previously described (41). Each condition was set up in duplicate wells and compared to cultures with T_eff alone. Data are means + SEM for $n = 4$ healthy individuals. Statistical difference between nonexpanded and expanded T_regs was determined by t test, where the difference seen at 1:2 is $P = 0.0050$, 1:4 is $P = 0.0025$, and 1:8 is $P = 0.0354$ (*$P < 0.05$ and **$P < 0.01$). (**D**) Suppression assays using CFSE-labeled CD4$^+$CD127$^+$CD25$^-$ cells sorted from standard peripheral blood mononuclear cells (PBMCs) as T_effs cultured alone or activated with anti-CD3/anti-CD28–coated beads and/or co-incubated with T_regs (from patients enrolled in this trial) show a consistent level of suppression. Comparison of mean of % proliferating CFSE$^+$ cells with increasing ratio of T_reg/T_eff is shown for nonexpanded T_reg as compared to expanded T_reg ($n = 3$). Statistical difference between nonexpanded and expanded T_regs from T1D patients was determined by t test, where the difference seen at 1:8 is $P = 0.0195$, 1:16 is $P = 0.0112$, and 1:32 is $P = 0.0333$ (*$P < 0.05$). (**E**) T_reg functional markers CD25, CD39, CD45RA, CD45RO, CTLA-4, and LAP were analyzed on expanded T_regs (solid squares) and nonexpanded T_regs (open circles) from the same healthy control donor by flow cytometry ($n > 4$ individuals as depicted). Representative plots from the FACS analysis can be seen in fig. S7. Significance was determined by t test.

No opportunistic infections or malignancies were observed. One subject developed grade 2 pharyngitis and had low-copy number cytomegalovirus (CMV) detected on day 7, but not detected at day 28, due to a presumed new infection with CMV occurring before receiving cells. There was no apparent relationship between adverse events and T_reg dose (table S2). The full listing of adverse events is in tables S3 to S6.

Metabolic results

Metabolic function was evaluated by measuring the C-peptide area under the curve (AUC) during an MMTT (Fig. 4). The C-peptide responses were generally unchanged at 1 year and even after 2 years in dose cohorts 1 and 2. Three of four subjects in cohort 3 and three of the four subjects in cohort 4 showed a decline in C-peptide of more than 50% over 78 weeks of follow-up. Two of four subjects in cohort 4 also had a decline in C-peptide of more than 50% over 52 weeks of follow-up; however, the remaining two patients remained stable from week 13 to 52 weeks. The heterogeneity of diabetes progression and the dependence of progression on age and on duration of diabetes do not allow us to draw a conclusion from these findings in a small number of subjects. The HbA1c levels remained stable in all but one subject in cohort 4, 007-103, whose levels went from 6.2% at screening to 12.6% at week 13, with the individual's C-peptide diminishing from 0.49 at screening to 0.249 pmol/ml at week 13. Insulin use was generally stable. In summary, there were too few subjects to make a clear statement about stabilization or decay in C-peptide in treated subjects. However, we note that 7 of 14 patients had a C-peptide reduction of <10% of baseline C-peptide, predominantly in the lower-dose group, whereas 7 of 14 showed an increase in C-peptide decline at 1 year (predominantly in the higher-dose cohorts). Given the small number of subjects in each cohort, the overall changes in C-peptide in this study fall within the expected decline observed in the natural history of the disease (30).
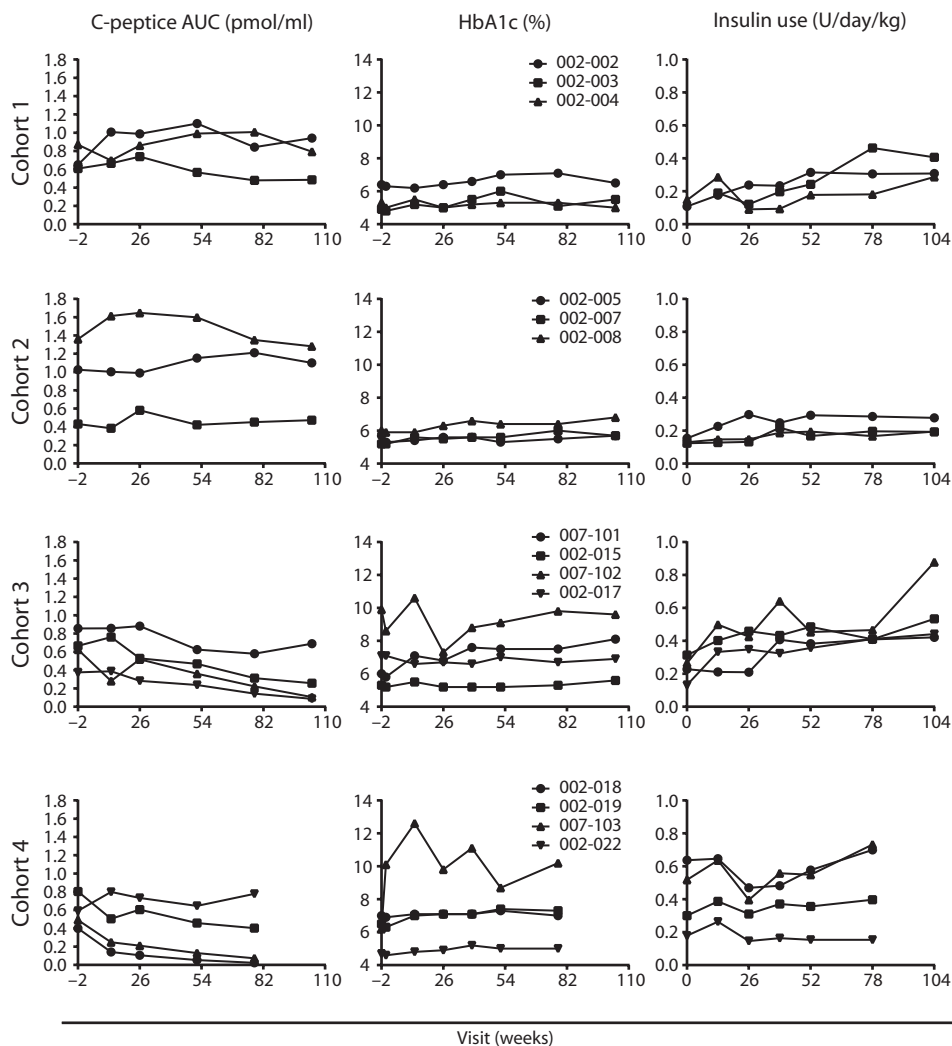
T lymphocyte subsets

We compared T lymphocyte subsets among participants who had been treated with polyT_regs before and after AT. Overall, consistent changes in T cell markers were not observed between

T_{reg}-treated patients after AT when compared to pretreatment. A small, transient increase in $CD38^+$ memory T cells was seen in the first week (Fig. 5A). A longer, more pronounced increase was seen in the percentage of $CCR7^+$ T_{regs} out to day 91 (Fig. 5B). In addition to these changes in T cell marker, an increase in CD25 median fluorescence intensity (MFI) of the T_{reg} population was seen on day 7 after infusion (Fig. 5C). All of these changes most likely represent the detection of the transferred polyT$_{reg}$ population. There was also a significant decrease in $CD56^{hi}CD16^{lo}$ natural killer (NK) cells early after poly-T$_{reg}$ injection among all patients enrolled, consistent with the reduction of a more pathogenic type 1 IFN-γ/tumor necrosis factor (TNF)–producing NK population (fig. S3) (31). We did not find a statistically significant change in the titers of anti-GAD65 (glutamic acid decarboxylase 65) or anti-ICA512 (islet cell autoantibody 512) antibodies or differences between the treatment groups.

Tracking the adoptively transferred expanded polyT$_{regs}$

Previous studies of allogeneic adoptive T_{reg} immunotherapy have shown the T_{regs} to be short-lived (32). Initial studies were performed to examine whether the adoptively transferred cells could be visualized on the basis of the cell surface expression profile of the expanded T_{regs}. There was a short-term increase in the percentage of CD25 bright cells (fig. S4). In addition, the MFI of CD25 of $CD4^+CD127^{lo}CD25^+$ cells increased from 385 ± 79 on day 0 to 859 ± 183 on day 1 and stayed up until day 7 (Fig. 5C). We developed a tool to monitor the adoptively transferred cells. T_{regs} were nonradioactively tagged by labeling the deoxyribose moiety of newly replicated DNA during expansion ex vivo, by metabolic labeling of cells with $[6,6-^2H_2]$glucose. This enabled tracking to be performed on the whole T_{reg} population in cohorts 3 and 4. As described in Materials and Methods, $[6,6-^2H_2]$glucose was added to the T_{reg} culture throughout the 14-day expansion. The $^2H_2$ (deuterium) label was incorporated into replicating DNA such that $59.8 \pm 1.03\%$ (SD) of the deoxyribose in purine deoxyribonucleosides isolated from cellular DNA was labeled in the expanded T_{regs} (range, 58.2 to 60.9%). The labeled cells were transferred into the patients, and blood samples were harvested at various time points after administration. T_{regs} sorted from purified PBMCs, AT, were analyzed for deuterium enrichment in the DNA (Fig. 6 and fig. S5). As seen in Fig. 6 (inset), at day 1, there was a significant percentage of deuterium label in the DNA of circulating
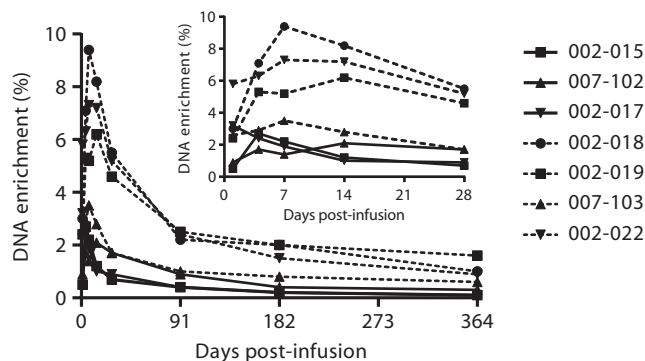
T_{regs} in each individual (Fig. 6, inset). The maximal percentage of the AT polyT$_{regs}$ occurred by 7 to 14 days, after which point there was a decline in the percentage of labeled T_{regs} in the circulation. Thus, by ~90 days after infusion, about 25% of the peak labeling in cells was still observed in the circulation. This percentage stabilized over the next 9 months, resulting in the prolonged presence of labeled T_{regs} in the circulation at least 1 year after transfer. Our pharmacokinetic analysis of the survival of the T_{regs} indicated a two-phase decay curve, with the average half-life of the fast decay phase of about 19.6 days (range, 4.7 to 32.5 days) and a second slow decay phase with a half-life of a year or more in four of seven patients studied (fig. S5 and table S7).

Fig. 4. Metabolic assessments. (**Left column**) C-peptide AUC. C-peptide AUC is reported for fasting 4-hour MMTT without carbohydrate restriction for 3 days preceding test. The target glucose level at the start of the test was between 70 and 200 mg/dl. Regular insulin or short-acting insulin analogs were allowed up to 6 and 2 hours before the test, respectively, to achieve the desired glucose level. The baseline blood samples (−10 and 0 min) were drawn, and then subjects drank Boost High Protein Nutritional Energy Drink (Nestle Nutrition) at 6 kcal/kg (1 kcal/ml) to a maximum of 360 ml. Blood was drawn at 15, 30, 60, 90, 120, 150, 180, 210, and 240 min after Boost dose. C-peptide AUC was calculated using the trapezoid rule. (**Middle column**) HbA1c. (**Right column**) Insulin use. Subjects self-reported insulin use for the 3 days immediately preceding the scheduled visit. The average total insulin (long acting + short acting) use per day normalized to weight is reported.

Fig. 6. Survival of infused polyT$_{regs}$. During ex vivo expansion, the ^{2}H label from deuterated glucose ([^{2}H$_2$]glucose) contained in the cell culture medium is incorporated into the deoxyribose moiety in replicating DNA through the de novo purine nucleotide synthesis pathway. Three subjects (002-015, 007-102, and 002-017) were treated with a single dose of ^{2}H-labeled T$_{regs}$ at a target dose of 3.2×10^8 cells, and four subjects (002-018, 002-019, 007-103, and 002-022) were treated with a target dose of 26×10^8 cells that were about 60% enriched for the ^{2}H label. Peripheral blood was collected on days 1, 4, 7, 14, 28, 91, 182, and 364 days after infusion, and T$_{regs}$ were sorted from the peripheral blood. After isolation and hydrolysis of genomic DNA, the ^{2}H isotopic enrichment of the purine deoxyribonucleosides in T$_{regs}$ sorted from whole blood was assessed by gas chromatography–mass spectrometry (GC-MS). Background enrichment of unlabeled T$_{regs}$ was ≤0.1% for each of the seven subjects.

There are several possible reasons for the decrease in the number of circulating T$_{regs}$, including cell death, migration to lymphoid tissues and inflammatory sites such as the pancreas, or a high degree of proliferation, thus diluting out the deuterium label. The current study design and data cannot distinguish among these possibilities. It also remained possible that the cells changed their T$_{reg}$ phenotype and the label was not captured in the sorting strategy for T$_{regs}$. To address this last possibility, we sorted all the CD4$^+$ cells not in the T$_{reg}$ gate and separated them into naïve, central memory, and effector memory subsets based on the expression of CD45RO and CD62L to see whether deuterium label was found in CD4$^+$ T cell other than T$_{regs}$ (fig. S6). At no time, up to 365 days, was any deuterium observed in any other subset other than bona fide T$_{regs}$ within the detection limit of 0.1% (Table 5). Because the labeling level of T$_{regs}$ ranged from 2 to 8% early and 1 to 2% later, if some fraction of T$_{regs}$ were converted to T$_{effs}$, then the relative contribution from T$_{regs}$ to any other pool would have to be less than 1:20 to 1:80 early and less than 1:10 to 1:20 later, suggesting that conversion of T$_{regs}$ into T$_{effs}$ could have occurred as a rare event, below the level of detection. Overall, the data suggest that the infused T$_{regs}$ did not transdifferentiate into T$_{effs}$.

However, there were indeed some changes in the phenotype of the infused T$_{regs}$. As mentioned above, the expanded polyT$_{regs}$ converted to a nearly uniform CD45RA$^-$CD45RO$^+$CCR7$^+$CD38^{high} phenotype during ex vivo expansion (Fig. 2). To test the stability of these markers, CD4$^+$CD127$^{lo/-}$CD25$^+$ T$_{regs}$ were further divided into separate subsets based on CD45, CCR7, and CD38 expression at various time points before and after infusion and then measured for deuterium enrichment as described above. Although most of the label within the T$_{regs}$ began in the CD45RA$^-$CD45RO$^+$CCR7$^+$CD38^{high} subset, we found that over time most of the T$_{reg}$-specific label was no longer in this subset

Fig. 5. Changes in T lymphocyte subsets after T$_{reg}$ infusion. PBMC samples collected from subjects on days 0, 7, 28, and 91 were frozen from all patients and then thawed simultaneously before being stained with CD4, CD45RO, CD25, CD127, CCR7, and CD38 for FACS analysis. Representative FACS plots for all analyses are shown in fig. S6. All subjects shown are from cohort 4 ($n = 4$), as detailed in Table 1. (**A**) An increase in % CD38$^+$ cells was seen within CD4$^+$CD45RO$^+$ T cell subset after T$_{reg}$ infusion. (**B**) Within the CD4$^+$CD127$^{lo/-}$CD25$^+$ T$_{regs}$, the percentage of CCR7$^+$ T$_{regs}$ increased after infusion of expanded T$_{regs}$. (**C**) MFI of the patients' CD4$^+$CD127$^{lo/-}$CD25$^+$ T$_{reg}$ population increased upon addition of expanded T$_{regs}$. For all plots, comparisons were made to day 0 and significance was determined by paired t test.

Table 5. Stability of infused polyT$_{regs}$. To address long-term stability of the infused expanded T$_{regs}$, samples collected on days 91 (in three of four patients only), 182, and 365 were sorted into T$_{reg}$ and non-T$_{reg}$ subsets as shown in fig. S6. Subsets were then analyzed by MS for ^{2}H label, which was incorporated into the infused T$_{regs}$ during the expansion. Values shown are % enrichment for ^{2}H and have an error of ±0.1.

Cell subset	DNA enrichment (%)										
	C012 (002-018)		C013 (002-019)			C014 (007-103)			C016 (002-022)		
	Day 182	Day 365	Day 91	Day 182	Day 365	Day 91	Day 182	Day 365	Day 91	Day 182	Day 365
T$_{regs}$											
CD4$^+$CD25$^+$CD127^{lo}	2.0	1.0	2.5	2.0	1.6	1.0	0.8	0.6	2.4	1.5	0.9
Non-T$_{regs}$											
CD45RO$^+$	0.0	0.0	0.0	0.0	0.0	0.0	0.0	0.0	0.0	0.0	0.0
CD45RO$^+$CD62L^{hi}	0.0	0.0	0.0	0.0	0.0	0.0	0.0	0.0	0.0	0.0	0.0
CD45RO$^+$CD62L^{lo}	0.1	0.0	0.0	0.0	0.0	0.0	0.0	0.0	0.0	0.0	0.0
CD45RO^{lo}CD62L^{hi}	0.0	0.0	0.0	0.0	0.0	0.0	0.0	0.0	0.0	0.0	0.0

(Fig. 7A). Although most of the deuterium-labeled T$_{regs}$ retained high levels of CCR7 expression (97 to 100%), there was clear evidence that most of the transferred cells lost CD38 expression and there was a switch from CD45RO to CD45RA (Fig. 7, B and C). The fact that the cells regained CD45RA expression could represent either a return to a resting naïve phenotype or a memory phenotype similar to that seen in a subset of CD8$^+$ and CD4$^+$ central memory T cells (*33*).
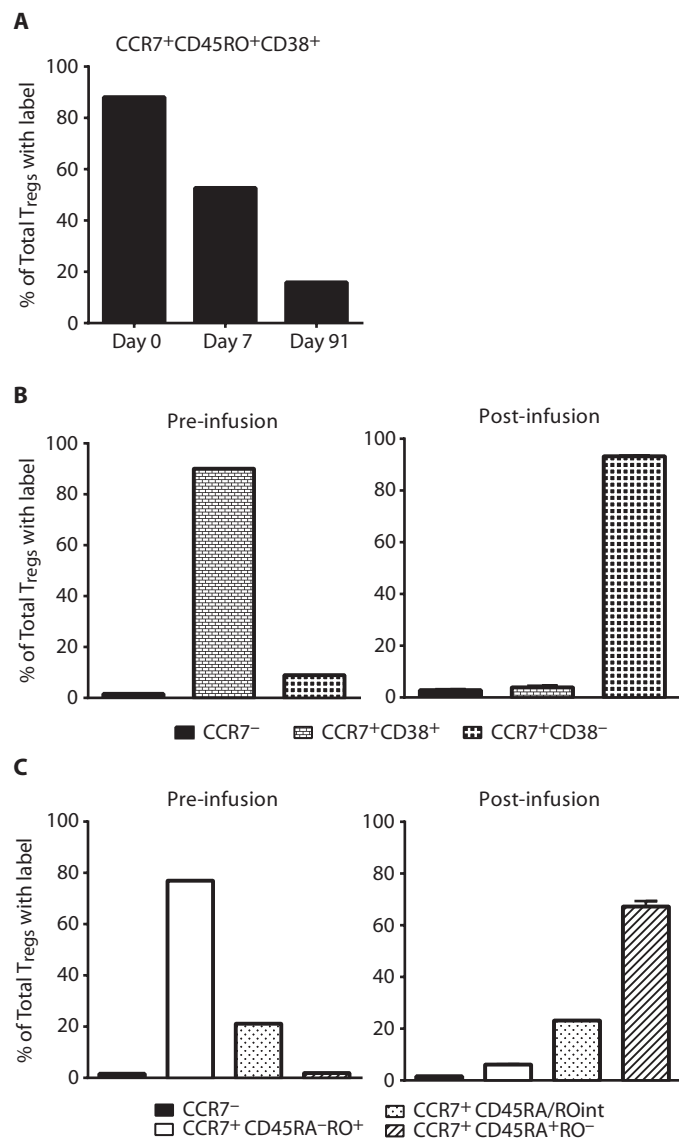
DISCUSSION

Several reports have described abnormalities in the functions of T$_{regs}$ in patients with T1D, such as impaired responses to IL-2, a critical factor normally needed for T$_{reg}$ growth and survival. Our group also described instability manifest by their expression of pathologic cytokines, suggesting that ex vivo T$_{reg}$ expansion and repair might re-regulate the autoimmunity (*34*). In nonobese diabetic (NOD) mice, our studies have shown that antigen-specific diabetogenic pathologic T cells may include some cells that have expressed FOXP3 during their development, raising the possibility that the unstable T$_{regs}$ may acquire pathologic function as a result of acquired factors. Clinical studies with exogenous IL-2 have indicated that expanding T$_{regs}$ can prevent autoimmunity, but in addition, repair of functional abnormalities is an important part of using these cells therapeutically. Here, we have expanded polyT$_{regs}$, evaluated their function, and tested their safety after reinfusion in patients with recent-onset T1D. A key achievement to accomplish this was our ability to expand the cells to sufficient numbers for in vivo therapy. Our culture methods and analysis of the expanded cells indicated that the expanded T$_{regs}$ were not contaminated with significant numbers of T$_{effs}$. Furthermore, we have illustrated that FOXP3 expression by FACS directly correlated with percent TSDR demethylation, indicating that the FOXP3$^+$ expression in these cells was stable after the 14-day ex vivo expansion period. The expanded T cells showed robust function in suppression assays in vitro and also corrected the defective pSTAT5 responses to IL-2.

The T$_{reg}$ infusions were well tolerated, and the results of this safety study suggest that the infusions are safe over a more than 500-fold dose range. Cytokine release, infusion reactions, or infectious complications were not seen. We also showed that the infused T$_{regs}$ did not acquire pathologic phenotypes. The AT T$_{regs}$ reexpressed CD45RA. It is likely that the changes from CD45RA to CD45RO during expansion were transient in nature. However, it is noteworthy that although central memory T cells are CD45RO$^+$CD45RA$^-$, effector memory T cells express CD45RA (*33*), suggesting that this change in phenotype for the AT T$_{regs}$ may reflect further engagement of antigen in vivo and the development of a distinct T$_{reg}$ memory population.

In addition to demonstrating the long life span of a subset of T$_{regs}$, the kinetic modeling results may have clinical implications. First, the calculated whole body pool size of T$_{regs}$ varied widely among T1D subjects. It will be of interest in future studies to determine whether this quantitative metric correlates with immune function or disease progression in individuals. Second, it will also be of interest to determine whether the relative proportion of T$_{regs}$ that were short- or long-lived (range, 75 to 90% short-lived) has functional importance in T$_{reg}$ AT and whether this kinetic behavior is a feature of the host subject.

Our studies of the T$_{reg}$ pharmacokinetics, based on reinfusion of T$_{regs}$ labeled ex vivo with stable isotopes, showed a delay in maximal AT T$_{regs}$ in the circulation and a two-phase decline curve that raises several questions. Other studies have suggested that the delay may be due to regulation of certain adhesion or homing receptors on the ex vivo–expanded T$_{regs}$ that prevent the cells from immediately entering the circulation but rather promote homing and lodging in the liver or lung for some period of time (*35*). The apparent precipitous decline in circulating AT polyT$_{regs}$ number between the first and third month after transfer may be due to cell death, perhaps due to a decrease in IL-2 signaling when shifting from the in vitro milieu to in vivo. Consistent with this possibility, on day 1, we observed a significant increase in CD25$^+$ T$_{regs}$ in the circulation, but this increased CD25 expression diminished rapidly, likely due to the reduced levels of IL-2 over time and perhaps leading to cell death (fig. S4). It should be pointed out that the increase in the percentage of CD25 bright T$_{regs}$ at day 1 may not fully reflect the presence of AT polyT$_{regs}$ entering the circulation because the relative percentages are higher than might have been expected based on the deuterium labeling. It would appear that the transfer of the ex vivo–expanded T$_{regs}$ might have carried over some IL-2 bound to the receptor that induced IL-2 receptor (IL-2R) on the endogenous T$_{regs}$.

A

CCR7⁺CD45RO⁺CD38⁺

B

Pre-infusion — Post-infusion

■ CCR7⁻   ▦ CCR7⁺CD38⁺   ▦ CCR7⁺CD38⁻

C

Pre-infusion — Post-infusion

■ CCR7⁻
□ CCR7⁺ CD45RA⁻RO⁺
▨ CCR7⁺ CD45RA/ROint
▨ CCR7⁺ CD45RA⁺RO⁻

Fig. 7. Changes in T_{reg} phenotypes after transfer. Frozen samples of expanded T_{regs} or PBMCs collected at time points on days 7 to 91 after infusion were FACS-sorted for $CD4^+CD25^+CD127^{lo}$ T_{regs}. These T_{regs} were further subsetted and sorted based on expression of CCR7, CD38, CD45RA, and CD45RO. Collected T_{reg} subsets were then analyzed by MS for ^2H label, which was incorporated into the infused T_{regs} during the expansion. (**A**) $CCR7^+CD45RO^+CD38^+$ T_{regs} (black bars) were analyzed for % enrichment, which represented an increasingly smaller proportion of total T_{reg} ^2H enrichment over time. (**B**) T_{regs} were subsetted into $CCR7^-$ (black bars), $CCR7^+CD38^+$ (small grid bars), and $CCR7^+CD38^-$ (large grid bars) populations for ^2H enrichment analysis before and after infusion. (**C**) T_{regs} were subsetted into $CCR7^-$ (black bars), $CCR7^+CD45RA^-CD45RO^+$ (white bars), $CCR7^+CD45RA^{int}CD45RO^{int}$ (speckled bars), and $CCR7^+CD45RA^+CD45RO^-$ (striped bars) populations for ^2H enrichment analysis before and after infusion. All plots shown are representative of data collected from subjects in cohort 4. "% of Total T_{regs} with Label" is defined in fig. S8.

The improvement in T_{reg} function and reversibility of the reduced pSTAT5 suggest that this aspect of T_{reg} function may be amenable to repair at least in the short term and in the context of in vitro expansion,

consistent with what was observed in the IL-2/rapamycin study (25). The reduction in pSTAT5 seen in T1D $CD4^+$ T cells reflects several polymorphisms found in the IL-2R and PTPN2, both of which are risk alleles for T1D. However, it may also in part reflect the absence of availability of IL-2 in patients at the time of diagnosis, possibly by consumption by other T_{effs}. Longer-term studies and analyses of the time of onset of this abnormality may help to resolve these questions. Despite the improvement in pSTAT5, we did not find that the cell culture process increased production of cytokines, such as IL-10, by the expanded T_{regs}, suggesting that some T_{reg} functions are not enhanced by in vitro expansion. In the future, further studies of the functional phenotype of the T_{regs} in vivo will address whether these additional functional activities have been enhanced.

Finally, there are several additional conclusions that can be drawn from the studies that have important implications. First, we have demonstrated that the expanded T_{regs} can be exported to other clinical sites, increasing the feasibility of developing this cell therapy into a true therapeutic. Second, although there were some phenotypic changes that occurred after T_{reg} infusion (such as CD38 and CD45R0 expression), the T_{regs} were overall quite stable for key parameters such as FOXP3, CD25, CD127 expression, and lack of T_{eff} cytokine production. However, it should be noted that we are only able to sample the cells in the circulation and there may be changes at the site in inflammation in the islets that are not evident when examining the blood. Finally, the enhanced suppressive activity seen in vitro under conditions of T_{reg} activation and expansion with IL-2 might suggest that there will be increased efficacy if the T_{regs} were combined with IL-2 therapy in vivo. This combination therapy is currently under development. In summary, we have shown that autologous T_{regs} can be expanded and are well tolerated in patients with recent-onset T1D. The expansion in vitro improves functional defects that have been identified in these cells in patients. Further adequately powered studies will be needed to determine whether the improvement in function and number leads to restoration of immunologic tolerance and prevention of disease progression.

There are several limitations to the study. As a phase 1 study, it was not powered to detect improvement in metabolic function, and therefore, we are unable to assess whether the improvement in the T_{regs} that we observed in vitro or the greater number of cells after AT will prevent progression of the autoimmune disease. However, the precipitous decline in C-peptide that had been described with high doses of IL-2, which expanded T_{regs} and NK cells in vivo, was not seen, and several of the patients in this phase 1 study had prolonged C-peptide production, especially in the lower-dose cohorts. Recently, Marek-Trzonkowska et al. reported initial findings of the infusion of T_{regs} in children with new-onset T1D (36, 37). Their approach to expansion of the cells had many similarities to ours, but they did not assess the effects of the culture on T_{reg} function. Moreover, the dosing that was used in that study was not fixed but given per kilogram, and additional doses were administered on the basis of deterioration in metabolic function—a late occurrence in disease progression. Nonetheless, these investigators suggested that the autologous T_{regs} might be able to maintain C-peptide responses. As with our study, they reported that the infusions were well tolerated without additional safety concerns, most notably no significant risk for infection. Another caveat in these studies is that analyses of the AT polyT_{regs} were limited to sampling of the peripheral blood, rather than the sites of autoimmune inflammation. Thus, issues such as local immune suppression, T_{reg} instability, and alteration of T_{effs} cannot be adequately addressed in this disease setting. Future studies in other

autoimmune diseases and organ transplantation should allow for tissue biopsies that can determine the local effects of polyT$_{reg}$ administration.

Thus, in summary, this study reports on the successful isolation, expansion, and reinfusion of polyT$_{regs}$ derived from patients with T1D. This provides a platform for additional clinical trials in this and other autoimmune diseases. The current efforts to use T$_{reg}$-promoting therapies, such as low-dose IL-2 (38), are likely to be complementary to this current AT effort, potentially resulting in a robust combination therapy, which, when combined with T$_{eff}$-depleting agents such as teplizumab and alefacept, may lead to durable remission and tolerance in this disease setting (39). Finally, efforts are under way to develop islet antigen–specific T$_{regs}$ using genetic engineering (chimeric antigen receptors and TCR transduction), which we and others have shown to be even more efficacious to treat autoimmune diabetes in animal models (16).

MATERIALS AND METHODS

Participants
This study enrolled male and female subjects diagnosed with T1D within 3 to 24 months of screening who were 18 to 45 years of age with peak C-peptide >0.1 pmol/ml during MMTT challenge, were positive for Epstein-Barr antibody, and were positive for at least one of the following antibodies: tyrosine phosphatase–related islet antigen 2 (IA-2), ICA, GAD65, insulin, and zinc transporter 8 (ZnT8). Subjects also had to have adequate venous access to support draw of 400 ml of whole blood and infusion of investigational therapy. Subjects were determined to be ineligible if they had hemoglobin <10.0 g/dl; leukocytes <3000/μl; neutrophils <1500/μl; lymphocytes <800/μl; platelets <100,000/μl; T$_{regs}$ <10/μl; evidence of active infection [HIV-1/HIV-2, hepatitis B, hepatitis C, Epstein-Barr virus (EBV) or CMV genomes, or positive purified protein derivative (PPD) skin test]; chronic use of systemic glucocorticoids or other immunosuppressive agents or biologic immunomodulators within 6 months before study entry; history of malignancy except adequately treated basal cell carcinoma; or any chronic illness or previous treatment that, in the opinion of the investigator, should preclude participation in the trial. Pregnant or breastfeeding women were excluded from the study, as well as any female who was unwilling to use a reliable and effective form of contraception for 2 years after T$_{reg}$ dosing, and any male who was unwilling to use a reliable and effective form of contraception for 3 months after T$_{reg}$ dosing. All participants provided written informed consent before participating in any study procedures.

T$_{reg}$ isolation and expansion (40)
About 400 ml of fresh peripheral blood was collected into blood pack units containing citrate phosphate dextrose (Fenwal) and processed within 24 hours for isolation of PBMCs via Ficoll density gradient (GE Healthcare Bio-Sciences). For subjects enrolled at Yale, blood was shipped to UCSF for processing in the good manufacturing practice (GMP) laboratory, and the expanded polyT$_{regs}$ were shipped back to Yale for infusion.

T$_{regs}$ were isolated on a BD FACSAria II high-speed cell sorter housed in a class 10,000 clean room with the following GMP-grade lyophilized antibodies: CD4-PerCP (peridinin chlorophyll protein) (L200), CD127-PE (phycoerythrin) (40131), and CD25-APC (allophycocyanin) (2A3)

(BD Biosciences). The sorted CD4$^+$CD127$^{lo/-}$CD25$^+$ T cells were collected into 3 ml of X-VIVO 15 medium (Lonza, catalog no. 04-418Q) containing 10% human heat-inactivated pooled AB serum (Valley Biomedical). T$_{reg}$ populations were analyzed for purity after sort and determined to be 98.4% (range, 96.3 to 99.6%) CD4$^+$CD127$^{lo/-}$CD25$^+$ T cells.

FACS-isolated cells were plated at ~2.5 × 10^5 T$_{regs}$ per well in multiple wells of a 24-well plate (Nunc) and activated with Dynabeads CD3/CD28 CTS anti-CD3/anti-CD28–coated microbeads (Life Technologies) at a 1:1 bead/cell ratio. Cells were cultured either in X-VIVO 15 or in X-VIVO 15 customized by Lonza by substituting 100% of the glucose in the base medium with D-glucose ([6,6-^{2}H$_2$], 99%) (Cambridge Isotope Laboratories, catalog no. DLM-349-MPT) supplemented with 10% human heat-inactivated pooled AB serum. At day 2, the culture volume was doubled and IL-2 was added (Proleukin, 300 IU/ml; Prometheus). Cells were resuspended, fresh medium and IL-2 were added at days 5, 7, 9, and 12, and the cells were transferred to cell culture plates and flasks (Nunc), and/or bags (Saint-Gobain) of increasing size to maintain a seeding density of ~2 × 10^5 to 3 × 10^5 cells/ml in plates or flasks and a concentration of 500,000/ml in bags. On day 9, cells were restimulated with fresh anti-CD3/anti-CD28–coated beads at a 1:1 ratio. On day 14, cells were consolidated and debeaded using a MaxSep magnet, and bead removal was verified via flow cytometry. Briefly, Dynabeads CD3/CD28 CTS (Invitrogen, catalog no. 402.03D) and Spherobeads (BD, catalog no. 556291) were used as controls for determining instrument settings and defining Dynabeads gate based on forward scatter (FSC) versus side scatter (SSC) followed by FL2 versus FL3 channels on FACSCalibur. Triplicate samples of expanded CD4$^+$CD127$^{lo/-}$CD25$^+$ T$_{regs}$ at ~5 × 10^6 cells/ml were analyzed, and a number of cells and Dynabeads in each sample were collected to determine cell number and bead number contained within each sample. The average bead count and average cell count were used to calculate the bead/cell ratio.

The product was prepared as a cell suspension of fresh, noncryopreserved cells in sterile infusion solution composed of 1:1 PlasmaLyte A/5% dextrose, 0.45% NaCl (Baxter) containing 0.5% human serum albumin (HSA) (Grifols), all supplied as U.S. Food and Drug Administration–approved drugs (PlasmaLyte A and dextrose/NaCl) or licensed products (HSA) for injection and conforming to U.S. Pharmacopeial Convention (USP) standards.

Administration and follow-up
Results of blood chemistries and hematology were reviewed, and a history of any recent illness or fever was obtained before infusion of the cells. Patients received premedication with acetaminophen and diphenhydramine. PolyT$_{regs}$ were infused via a peripheral intravenous line over 10 to 30 min. Vital signs were taken before and after infusion, then every 15 min for at least 1 hour, then every hour for the first 4 hours, and every 4 hours for 20 hours. Chemistries and complete blood count with differential blood count were repeated the next day before discharge from the clinical research unit. Patients were seen for follow-up assessments on day 4 after infusion, then weekly for 4 weeks, then every 13 weeks for 1 year, and then every 26 weeks for 2 years. Telephone monitoring for adverse events continues every 6 months for 5 years after infusion followed by a final clinic visit.

Phenotypic analysis of expanded T$_{reg}$ populations and peripheral blood samples
Freshly expanded cells were evaluated for expression of CD4, CD25, CD127, CD8 (BD Biosciences), and FOXP3. Intracellular staining was

performed with Alexa 488–conjugated anti-FOXP3 (clone 206D) and the FOXP3 staining kit (BioLegend) according to the manufacturer's instructions and modified as follows: 2×10^6 cells were washed and fixed for 30 min at room temperature using fixation/permeabilization buffer. Cells were washed, resuspended in perm buffer containing deoxyribonuclease I (100 U/ml; Sigma-Aldrich), and incubated for 30 min at room temperature, followed by two washes in perm buffer. Cells were subsequently blocked with human immunoglobulin G (IgG) (5 μg per test) for 5 min and stained for cell surface and intracellular markers along with anti-human FOXP3–Alexa 488 (5 μl per test) or isotype control. Flow cytometric data were collected on a FACSCalibur cytometer (BD Biosciences) and analyzed with FlowJo software (version 9; Tree Star). In experiments to determine phenotype of expanded T_{regs} and localization of the deuterium labeling, antibodies used for flow cytometric sorting on a BD FACSAria II cytometer included CD45RA-APC (H100) (BioLegend), CD4–Alexa 488 (RPA-T4) (Becton Dickinson), CD38-PerCP-Cy5.5 (HIT2) (BioLegend), CCR7-V450 (150503) (Becton Dickinson), CD45RO-PE-Cy7 (UCHL1) (BioLegend), CD127-PE (hIL-7R-M21) (Becton Dickinson), and CD25-BV786 (M-A251) (Becton Dickinson). FACS files were analyzed with FlowJo software version 9 or greater.

Studies of clinical samples conducted at the Benaroya Research Institute (BRI) were performed as follows. PBMCs collected at baseline and throughout the study were frozen for batched analysis. These PBMC samples were subsequently thawed, labeled, and analyzed as previously described (25) for STAT5 signaling and the immunophenotyping of lymphocyte and T cell subsets. Multicolor flow cytometry was conducted on a BD LSRII flow cytometer and analyzed in FlowJo using standardized panels developed by the Immune Tolerance Network (www.immunetolerance.org).

For studies of nonclinical samples at the BRI, cells (nonexpanded T_{regs} or D14-expanded T_{regs} from the same donor) were suspended in FACS buffer [phosphate-buffered saline + 1% fetal bovine serum (FBS) + 0.1% NaN_3]. To block Fc receptor–mediated binding of antibodies, cells were suspended in FACS buffer with 1% human serum (MP Biomedicals) for 20 min. These cells were washed, placed on ice for 30 min, and stained with cell surface fluorochrome-conjugated anti-human CD3, CD4, CD45RA, CD45RO, PD-1, and LAP (BioLegend); anti-human CD4, CD25, and CD127 (BD Biosciences); and anti-CD39 (eBioscience). Intracellular staining for FOXP3 (BioLegend) and CTLA-4 (BD Biosciences) was performed using the manufacturer's protocol. Cells were washed twice in buffer and analyzed by BD LSRII flow cytometer. All data analyses were performed using FlowJo software.

Suppression assays

T_{reg} suppression was assessed by measuring proliferation based on either a [^{3}H]thymidine incorporation or CFSE dilution assay. [^{3}H]-thymidine incorporation T_{reg} suppression assays were performed after expansion for all 14 individuals enrolled in the clinical trial as previously described (20), with the addition of a standard expanded T_{reg} population in each assay to ensure that the data were comparable and could be combined. For all control subjects, suppression was assessed on the basis of CFSE dilution as analyzed by flow cytometry as previously described (41). In brief, CFSE-labeled autologous $CD4^+$ $CD25^-$ T_{effs} were cocultured in round bottom plates with or without expanded T_{regs} or $CD4^+CD25^{hi}CD127^{lo/-}$ T_{regs} sorted from freshly isolated PBMCs and activated with Dynabeads human T activator CD3/CD28 (Invitrogen) for 4 days. Varying ratios of T_{eff}/T_{reg} were plated in

duplicate or triplicate. For comparisons of clinically expanded T_{regs} to nonexpanded T_{regs} from the same subject, a small-scale version of the previously described CFSE suppression assay was used, where T_{effs} were plated at 10,000 cells per well at a 1:10 bead/T_{eff} ratio. For the small-scale CFSE suppression assays, all T_{regs} were isolated from cryopreserved material and in vitro suppression was assessed on the basis of T_{reg} capacity to suppress the proliferation of a standard allogeneic responder T cells generated from a healthy donor whose PBMCs were cryopreserved in multiple aliquots containing 10×10^6 cells per vial. Additionally, standard nonexpanded T_{reg} and expanded T_{reg} populations were included in each assay to ensure that the data were comparable and could be aggregated.

In vitro suppression assays were performed in RPMI 1640 (Mediatech) supplemented with 5 mM Hepes, 2 mM L-glutamine, penicillin/streptomycin (50 μg/ml each) (Invitrogen), 50 μM 2-mercaptoethanol (Sigma), 5 mM nonessential amino acids, 5 mM sodium pyruvate (Mediatech), and 10% FBS (Omega Scientific). Cultures were maintained in 200-μl volumes in U-bottom 96-well plates (Costar) incubated at 37°C and 5% CO_2.

Cytokine analysis

T_{regs} were assessed for cytokine production at day 14 of culture via intracellular staining. Intracellular cytokines were stained directly from cultures at day 14 or after 4 hours of reactivation with anti-CD3/anti-CD28–coated beads or PMA/ionomycin. Intracellular cytokine staining was conducted with FOXP3 staining using the manufacturer kit reagents from BioLegend as previously described along with the anti-human cytokine antibodies IFN-γ–PE and IL-10–APC (Becton Dickinson).

TCRβ repertoire analysis

Genomic DNA was extracted from 2.5×10^5 freshly isolated T_{regs} and 1×10^6 ex vivo–expanded polyT_{regs}. The DNA was submitted to Adaptive Biotechnologies for deep-level TCRβ sequencing. TCR gene frequency analysis was performed using algorithms developed by Adaptive Biotechnologies.

TSDR methylation assay

Genomic DNA from 1×10^6 expanded T_{regs} was analyzed by Epiontis GmbH according to established protocol. Percentages of demethylated TSDR were calculated as follows: [mean copy numbers of unmethylated DNA/(mean copy numbers of unmethylated DNA + copy numbers of methylated DNA)] × 100. For female T_{regs}, the percentages calculated above were multiplied by 2 to correct for X-chromosome inactivation.

T_{reg} deuterium tracking

During the 14-day clinical expansion period, the $^2H_2$ label from [6,6-$^2H_2$]glucose in the X-VIVO 15 culture medium was incorporated into the DNA of replicating polyclonal $CD4^+CD127^{lo/-}CD25^+$ T_{regs} as previously described (42). Initial qualifying experiments showed no differences in fold expansions, phenotype, or percent TSDR demethylation between T_{regs} grown in X-VIVO 15 and T_{regs} grown in [$^2H_2$]glucose-containing X-VIVO 15. Functional suppression assay results showed similar inhibition between T_{regs} expanded in either type of medium, and cultures were free from bacteria, fungi, mycoplasma, or endotoxin contaminants. MS analyses showed that T_{regs} expanded in X-VIVO 15 with [6,6-$^2H_2$]glucose in the medium at 100% enrichment were ~60% enriched for $^2H_2$ in the deoxyribose moiety of purine deoxyribonucleotides isolated from DNA, which is the

theoretical maximum deuterium enrichment observed in deoxyribose in fully replaced cells that divided in the presence of [6,6-^{2}H$_2$]glucose (42, 43). This 60% enrichment level was consistently observed in all seven preparations in this clinical study.

After infusion of the labeled T$_{regs}$, peripheral blood was collected from the study participants, purified for T$_{regs}$, and analyzed for stable isotope enrichment. In some experiments, the cells were subdivided into T$_{reg}$ versus T$_{effs}$, as well as subsets of T$_{regs}$, to determine the stability of the T$_{reg}$ surface markers.

Analysis of DNA enrichment by MS

Measurement of deuterium in newly synthesized DNA was performed by GC-MS as described in detail previously (42). Briefly, DNA from proteinase K cell digests was isolated using DNeasy microcolumns (Qiagen) and hydrolyzed using S-1 nuclease and acid phosphatase. Deoxyribose moieties from purine dR-nucleosides were converted to pentafluorobenzylhydroxylamine triacetate derivatives. Enrichment analysis was performed on an Agilent 6890/5973 GC/MS equipped with a 30-m DB-17MS column (inside diameter, 250 μm; film thickness, 25 μm; Agilent) using methane negative chemical ionization and collecting ions in SIM mode at mass/charge ratios (m/z) 435, 436, and 437 (M0, M+1, and M+2, respectively). Enrichment of the [5,5-^{2}H$_2$]deoxyribose derivative was determined from measured ratios of the peak abundances of the M+2 ion to the sum of the M+0 to M+2 ions, after subtracting the theoretical (unenriched) natural abundance ratios, which are validated with standard curves of % enrichment.

Laboratory tests

Biochemical autoantibody titers were assayed at the Barbara Davis Center using radioimmunobinding assays, and ICA was measured at the University of Florida. C-peptide and HbA1c were measured at the Northwest Lipid Research Laboratory. Viral loads for EBV and CMV were performed by ViraCor Laboratories. Chemistries and hematology were performed at local clinical laboratories at UCSF and Yale.

Statistics and methods of analysis

Data analyses were performed using GraphPad Prism 6.0 software, and values at $P < 0.05$ were deemed significant. Cytokine concentrations were determined using SoftMax Pro software (Molecular Devices) with four-parameter data analysis.

SUPPLEMENTARY MATERIALS

www.sciencetranslationalmedicine.org/cgi/content/full/7/315/315ra189/DC1
Fig. S1. TCR repertoires of T$_{regs}$ before and after expansion.
Fig. S2. T$_{reg}$ function of expanded T$_{regs}$ from patients in phase 1 trial.
Fig. S3. Decreased CD56^{hi} NK cells in circulation after T$_{reg}$ infusion.
Fig. S4. Direct evidence for expanded T$_{regs}$ in the circulation after injection.
Fig. S5. Clearance of infused T$_{regs}$ exhibits biphasic exponential decay kinetics.
Fig. S6. Gating strategies for cell sorting and analysis of unfixed CD4$^+$ T cells and subsequent subsets.
Fig. S7. FACS-based phenotyping of nonexpanded and expanded FOXP3$^+$ T$_{reg}$.
Fig. S8. Equation for calculating "% of Total T$_{regs}$ with Label".
Table S1. Tabulation of cumulative number of adverse events for all cohorts categorized by system organ class and severity.
Table S2. Tabulation of cumulative number of adverse events categorized by cohort and severity.
Table S3. Listing of cumulative adverse events reported for cohort 1 by CTCAE term and severity.
Table S4. Listing of cumulative adverse events reported for cohort 2 by CTCAE term and severity.
Table S5. Listing of cumulative adverse events reported for cohort 3 by CTCAE term and severity.
Table S6. Listing of cumulative adverse events reported for cohort 4 by CTCAE term and severity.
Table S7. Two-phase decay model parameters.
Raw data for Fig. 2.
Raw data for Fig. 3B.
Raw data for Fig. 6.

REFERENCES AND NOTES

1. J. A. Bluestone, K. Herold, G. Eisenbarth Genetics, pathogenesis and clinical interventions in type 1 diabetes. *Nature* **464**, 1293–1300 (2010).
2. J. A. McKnight, S. H. Wild, M. J. E. Lamb, M. N. Cooper, T. W. Jones, E. A. Davis, S. Hofer, M. Fritsch, E. Schober, J. Svensson, T. Almdal, R. Young, J. T. Warner, B. Delemer, P. F. Souchon, R. W. Holl, W. Karges, D. M. Kieninger, S. Tigas, A. Bargiota, C. Sampanis, V. Cherubini, R. Gesuita, I. Strele, S. Pildava, K. J. Coppell, G. Magee, J. G. Cooper, S. F. Dinneen, K. Eeg-Olofsson, A.-M. Svensson, S. Gudbjornsdottir, H. Veeze, H.-J. Aanstoot, M. Khalangot, W. V. Tamborlane, K. M. Miller, Glycaemic control of Type 1 diabetes in clinical practice early in the 21st century: An international comparison. *Diabet. Med.* **32**, 1036–1050 (2015).
3. K. M. Miller, N. C. Foster, R. W. Beck, R. M. Bergenstal, S. N. DuBose, L. A. DiMeglio, D. M. Maahs, W. V. Tamborlane; T1D Exchange Clinic Network, Current state of type 1 diabetes treatment in the U.S.: Updated data from the T1D exchange clinic registry. *Diabetes Care* **38**, 971–978 (2015).
4. K. C. Herold, S. E. Gitelman, M. R. Ehlers, P. A. Gottlieb, C. J. Greenbaum, W. Hagopian, K. D. Boyle, L. Keyes-Elstein, S. Aggarwal, D. Phippard, P. H. Sayre, J. McNamara, J. A. Bluestone; AbATE Study Team, Teplizumab (anti-CD3 mAb) treatment preserves C-peptide responses in patients with new-onset type 1 diabetes in a randomized controlled trial: Metabolic and immunologic features at baseline identify a subgroup of responders. *Diabetes* **62**, 3766–3774 (2013).
5. M. R. Rigby, L. A. DiMeglio, M. S. Rendell, E. I. Felner, J. M. Dostou, S. E. Gitelman, C. M. Patel, K. J. Griffin, E. Tsalikian, P. A. Gottlieb, C. J. Greenbaum, N. A. Sherry, W. V. Moore, R. Monzavi, S. M. Willi, P. Raskin, A. Moran, W. E. Russell, A. Pinckney, L. Keyes-Elstein, M. Howell, S. Aggarwal, N. Lim, D. Phippard, G. T. Nepom, J. McNamara, M. R. Ehlers; T1DAL Study Team, Targeting of memory T cells with alefacept in new-onset type 1 diabetes (T1DAL study): 12 Month results of a randomised, double-blind, placebo-controlled phase 2 trial. *Lancet Diabetes Endocrinol.* **1**, 284–294 (2013).
6. M. J. Haller, S. E. Gitelman, P. A. Gottlieb, A. W. Michels, S. M. Rosenthal, J. J. Shuster, B. Zou, T. M. Brusko, M. A. Hulme, C. H. Wasserfall, C. E. Mathews, M. A. Atkinson, D. A. Schatz, Antithymocyte globulin/G-CSF treatment preserves β cell function in patients with established type 1 diabetes. *J. Clin. Invest.* **125**, 448–455 (2015).
7. J. C. Voltarelli, C. E. B. Couri, A. B. P. L. Stracieri, M. C. Oliveira, D. A. Moraes, F. Pieroni, M. Coutinho, K. C. R. Malmegrim, M. C. Foss-Freitas, B. P. Simões, M. C. Foss, E. Squiers, R. K. Burt, Autologous nonmyeloablative hematopoietic stem cell transplantation in newly diagnosed type 1 diabetes mellitus. *JAMA* **297**, 1568–1576 (2007).
8. Q. Tang, J. A. Bluestone, Regulatory T-cell therapy in transplantation: Moving to the clinic. *Cold Spring Harb. Perspect. Med.* **3**, a015552 (2013).
9. B. M. Hall, N. W. Pearce, K. E. Gurley, S. E. Dorsch, Specific unresponsiveness in rats with prolonged cardiac allograft survival after treatment with cyclosporine. III. Further characterization of the CD4$^+$ suppressor cell and its mechanisms of action. *J. Exp. Med.* **171**, 141–157 (1990).
10. S. Sakaguchi, N. Sakaguchi, M. Asano, M. Itoh, M. Toda, Immunologic self-tolerance maintained by activated T cells expressing IL-2 receptor α-chains (CD25). Breakdown of a single mechanism of self-tolerance causes various autoimmune diseases. *J. Immunol.* **155**, 1151–1164 (1995).
11. Q. Tang, J. A. Bluestone, The Foxp3$^+$ regulatory T cell: A jack of all trades, master of regulation. *Nat. Immunol.* **9**, 239–244 (2008).
12. R. Bacchetta, L. Passerini, E. Gambineri, M. Dai, S. E. Allan, L. Perroni, F. Dagna-Bricarelli, C. Sartirana, S. Matthes-Martin, A. Lawitschka, C. Azzari, S. F. Ziegler, M. K. Levings, M. G. Roncarolo, Defective regulatory and effector T cell functions in patients with *FOXP3* mutations. *J. Clin. Invest.* **116**, 1713–1722 (2006).
13. E. A. Green, L. Gorelik, C. M. McGregor, E. H. Tran, R. A. Flavell, CD4$^+$CD25$^+$ T regulatory cells control anti-islet CD8$^+$ T cells through TGF-β–TGF-β receptor interactions in type 1 diabetes. *Proc. Natl. Acad. Sci. U.S.A.* **100**, 10878–10883 (2003).
14. H. Waldmann, R. Hilbrands, D. Howie, S. J. Cobbold, Harnessing FOXP3$^+$ regulatory T cells for transplantation tolerance. *J. Clin. Invest.* **124**, 1439–1445 (2014).
15. J. A. Bluestone, E. Trotta, D. Xu, The therapeutic potential of regulatory T cells for the treatment of autoimmune disease. *Expert Opin. Ther. Targets* **19**, 1091–1103 (2015).
16. Q. Tang, K. J. Henriksen, M. Bi, E. B. Finger, G. Szot, J. Ye, E. L. Masteller, H. McDevitt, M. Bonyhadi, J. A. Bluestone, In vitro–expanded antigen-specific regulatory T cells suppress autoimmune diabetes. *J. Exp. Med.* **199**, 1455–1465 (2004).
17. Q. Tang, J. Y. Adams, C. Penaranda, K. Melli, E. Piaggio, E. Sgouroudis, C. A. Piccirillo, B. L. Salomon, J. A. Bluestone, Central role of defective interleukin-2 production in the triggering of islet autoimmune destruction. *Immunity* **28**, 687–697 (2008).

18. S. A. Long, K. Cerosaletti, P. L. Bollyky, M. Tatum, H. Shilling, S. Zhang, Z.-Y. Zhang, C. Pihoker, S. Sanda, C. Greenbaum, J. H. Buckner, Defects in IL-2R signaling contribute to diminished maintenance of FOXP3 expression in CD4⁺CD25⁺ regulatory T-cells of type 1 diabetic subjects. *Diabetes* **59**, 407–415 (2010).

19. W. Liu, A. L. Putnam, Z. Xu-Yu, G. L. Szot, M. R. Lee, S. Zhu, P. A. Gottlieb, P. Kapranov, T. R. Gingeras, B. Fazekas de St. Groth, C. Clayberger, D. M. Soper, S. F. Ziegler, J. A. Bluestone, CD127 expression inversely correlates with FoxP3 and suppressive function of human CD4⁺ T reg cells. *J. Exp. Med.* **203**, 1701–1711 (2006).

20. A. L. Putnam, T. M. Brusko, M. R. Lee, W. Liu, G. L. Szot, T. Ghosh, M. A. Atkinson, J. A. Bluestone, Expansion of human regulatory T-cells from patients with type 1 diabetes. *Diabetes* **58**, 652–662 (2009).

21. M. Nascimbeni, E.-C. Shin, L. Chiriboga, D. E. Kleiner, B. Rehermann, Peripheral CD4⁺CD8⁺ T cells are differentiated effector memory cells with antiviral functions. *Blood* **104**, 478–486 (2004).

22. S. K. Chauhan, D. R. Saban, T. H. Dohlman, R. Dana, CCL-21 conditioned regulatory T cells induce allotolerance through enhanced homing to lymphoid tissue. *J. Immunol.* **192**, 817–823 (2014).

23. J. Chen, Y.-G. Chen, P. C. Reifsnyder, W. H. Schott, C.-H. Lee, M. Osborne, F. Scheuplein, F. Haag, F. Koch-Nolte, D. V. Serreze, E. H. Leiter, Targeted disruption of CD38 accelerates autoimmune diabetes in NOD/Lt mice by enhancing autoimmunity in an ADP-ribosyltransferase 2-dependent fashion. *J. Immunol.* **176**, 4590–4599 (2006).

24. U. Baron, S. Floess, G. Wieczorek, K. Baumann, A. Grützkau, J. Dong, A. Thiel, T. J. Boeld, P. Hoffmann, M. Edinger, I. Türbachova, A. Hamann, S. Olek, J. Huehn, DNA demethylation in the human *FOXP3* locus discriminates regulatory T cells from activated FOXP3⁺ conventional T cells. *Eur. J. Immunol.* **37**, 2378–2389 (2007).

25. S. A. Long, M. Rieck, S. Sanda, J. B. Bollyky, P. L. Samuels, R. Goland, A. Ahmann, A. Rabinovitch, S. Aggarwal, D. Phippard, P. J. Bianchine, K. D. Boyle, S. A. Adah, J. A. Bluestone, J. H. Buckner, C. J. Greenbaum; Diabetes TrialNet and the Immune Tolerance Network, Rapamycin/IL-2 combination therapy in patients with type 1 diabetes augments Tregs yet transiently impairs β-cell function. *Diabetes* **61**, 2340–2348 (2012).

26. S. A. McClymont, A. L. Putnam, M. R. Lee, J. H. Esensten, W. Liu, M. A. Hulme, U. Hoffmüller, U. Baron, S. Olek, J. A. Bluestone, T. M. Brusko, Plasticity of human regulatory T cells in healthy subjects and patients with type 1 diabetes. *J. Immunol.* **186**, 3918–3926 (2011).

27. L. Hansmann, C. Schmidl, J. Kett, L. Steger, R. Andreesen, P. Hoffmann, M. Rehli, M. Edinger, Dominant Th2 differentiation of human regulatory T cells upon loss of FOXP3 expression. *J. Immunol.* **188**, 1275–1282 (2012).

28. K. L. Hippen, S. C. Merkel, D. K. Schirm, C. M. Sieben, D. Sumstad, D. M. Kadidlo, D. H. McKenna, J. S. Bromberg, B. L. Levine, J. L. Riley, C. H. June, P. Scheinberg, D. C. Douek, J. S. Miller, J. E. Wagner, B. R. Blazar, Massive ex vivo expansion of human natural regulatory T cells (T_regs) with minimal loss of in vivo functional activity. *Sci. Transl. Med.* **3**, 83ra41 (2011).

29. J. A. Bluestone, H. Bour-Jordan, M. Cheng, M. Anderson, T cells in the control of organ-specific autoimmunity. *J. Clin. Invest.* **125**, 2250–2260 (2015).

30. C. J. Greenbaum, C. A. Beam, D. Boulware, S. E. Gitelman, P. A. Gottlieb, K. C. Herold, J. M. Lachin, P. McGee, J. P. Palmer, M. D. Pescovitz, H. Krause-Steinrauf, J. S. Skyler, J. M. Sosenko; Type 1 Diabetes TrialNet Study Group, Fall in C-peptide during first 2 years from diagnosis: Evidence of at least two distinct phases from composite Type 1 Diabetes TrialNet data. *Diabetes* **61**, 2066–2073 (2012).

31. J. M. Milush, S. López-Vergès, V. A. York, S. G. Deeks, J. N. Martin, F. M. Hecht, L. L. Lanier, D. F. Nixon, CD56^neg CD16⁺ NK cells are activated mature NK cells with impaired effector function during HIV-1 infection. *Retrovirology* **10**, 158 (2013).

32. C. G. Brunstein, J. S. Miller, Q. Cao, D. H. McKenna, K. L. Hippen, J. Curtsinger, T. Defor, B. L. Levine, C. H. June, P. Rubinstein, P. B. McGlave, B. R. Blazar, J. E. Wagner, Infusion of ex vivo expanded T regulatory cells in adults transplanted with umbilical cord blood: Safety profile and detection kinetics. *Blood* **117**, 1061–1070 (2011).

33. H. T. Maecker, J. P. McCoy, R. Nussenblatt, Standardizing immunophenotyping for the human immunology project. *Nat. Rev. Immunol.* **12**, 191–200 (2012).

34. S. L. Bailey-Bucktrout, J. A. Bluestone, Regulatory T cells: Stability revisited. *Trends Immunol.* **32**, 301–306 (2011).

35. N. Meidenbauer, J. Marienhagen, M. Laumer, S. Vogl, J. Heymann, R. Andreesen, A. Mackensen, Survival and tumor localization of adoptively transferred melan-A-specific T cells in melanoma patients. *J. Immunol.* **170**, 2161–2169 (2003).

36. N. Marek-Trzonkowska, M. Myśliwiec, A. Dobyszuk, M. Grabowska, I. Derkowska, J. Juścińska, R. Owczuk, A. Szadkowska, P. Witkowski, W. Młynarski, P. Jarosz-Chobot, A. Bossowski, J. Siebert, P. Trzonkowski, Therapy of type 1 diabetes with CD4⁺CD25^high CD127-regulatory T cells prolongs survival of pancreatic islet—Results of one year follow-up. *Clin. Immunol.* **153**, 23–30 (2014).

37. N. Marek-Trzonkowska, M. Myśliwiec, A. Dobyszuk, M. Grabowska, I. Techmańska, J. Juścińska, M. A. Wujtewicz, P. Witkowski, W. Młynarski, A. Balcerska, J. Myśliwska, P. Trzonkowski, Administration of CD4⁺CD25^high CD127⁻ regulatory T cells preserves β-cell function in type 1 diabetes in children. *Diabetes Care* **35**, 1817–1820 (2012).

38. D. Klatzmann, A. K. Abbas, The promise of low-dose interleukin-2 therapy for autoimmune and inflammatory diseases. *Nat. Rev. Immunol.* **15**, 283–294 (2015).

39. M. R. Ehlers, M. R. Rigby, Targeting memory T cells in type 1 diabetes. *Curr. Diab. Rep.* **15**, 84 (2015).

40. A. L. Putnam, N. Safinia, A. Medvec, M. Laszkowska, M. Wray, M. A. Mintz, E. Trotta, G. L. Szot, W. Liu, A. Lares, K. Lee, A. Laing, R. I. Lechler, J. L. Riley, J. A. Bluestone, G. Lombardi, Q. Tang, Clinical grade manufacturing of human alloantigen-reactive regulatory T cells for use in transplantation. *Am. J. Transplant.* **13**, 3010–3020 (2013).

41. A. Schneider, J. H. Buckner, Assessment of suppressive capacity by human regulatory T cells using a reproducible, bi-directional CFSE-based in vitro assay. *Methods Mol. Biol.* **707**, 233–241 (2011).

42. D. C. Macallan, C. A. Fullerton, R. A. Neese, K. Haddock, S. S. Park, M. K. Hellerstein, Measurement of cell proliferation by labeling of DNA with stable isotope-labeled glucose: Studies in vitro, in animals, and in humans. *Proc. Natl. Acad. Sci. U.S.A.* **95**, 708–713 (1998).

43. R. Busch, R. A. Neese, M. Awada, G. M. Hayes, M. K. Hellerstein, Measurement of cell proliferation by heavy water labeling. *Nat. Protoc.* **2**, 3045–3057 (2007).

Editor's Summary

Regulating type 1 diabetes

In patients with type 1 diabetes (T1D), immune cells attack the insulin-producing β cells of the pancreas. The resulting prolonged increase in blood sugar levels can lead to serious complications including heart disease and kidney failure. Regulatory T cells (T_{regs}) have been shown to be defective in autoimmune diseases. Now, Bluestone *et al.* report a phase 1 trial of adoptive T_{reg} immunotherapy to repair or replace T_{regs} in type 1 diabetics. The ex vivo–expanded polyclonal T_{regs} were long-lived after transfer and retained a broad T_{reg} phenotype long-term. Moreover, the therapy was safe, supporting efficacy testing in further trials.

The following resources related to this article are available online at http://stm.sciencemag.org.
This information is current as of November 25, 2015.